

Flow Pattern and Velocity Distribution in a Spark Ignited Internal Combustion Engine

Y. Morita*, T. Sasahara* and K. Ohtake**

Toyohashi University of Technology, Tempaku-Cho, Toyohashi-Shi, 440

R.F. Sawyer***

University of California at Berkeley, Berkeley, CA 94720

ABSTRACT

Flow pattern and velocity distribution of charged gas into a cylinder of spark ignited internal combustion engine were measured by laser Doppler anemometer under the motoring conditions. A 250 ml, four-valved motorcycle air cooling engine was used. Time mean velocity and velocity fluctuation in the direction of piston stroke were measured and mapped on a distance along diameter and crank angle plane.

Engine speed, degree of throttle opening, single and dual valve suction operations were selected as the experimental conditions in order to get the fundamental data to simulate the relation between the engine performance and flow characteristics.

The higher the engine runs and the more the throttle is opened, the higher the velocity and the more uniform the flow pattern becomes. Within the experimental conditions, both the time mean flow velocity and the velocity fluctuation induced at the suction stroke had the tendency to be maintained during the compression stroke. An almost symmetric flow pattern appeared near the cylinder head at the dual valve operation, while asymmetric one did at the single valve. Flow pattern under this region was affected by the momentum of intake flow and showed a complicated characteristics. More intensive mixing is attained in the single valve operation at slow engine speeds and better combustion condition is realized.

INTRODUCTION

In order to design the high performance internal combustion engine or to understand the characteristics of combustion in it, a lot of efforts have been made to clarify the relation between the flow pattern and combustion phenomena. Flow visualization techniques with a transparent model engine and water flow system^{1),2)}, give us a quantitative explanations about the flow pattern inside the cylinder. Transparent square piston engines with combustion experiments observed by a photographic techniques³⁾ and combined with the

velocity measurements by hot wire^{4),5)}, and laser Doppler anemometers^{6),7),8)} have been tried to get the more quantitative data to understand the relation between flow characteristics and engine performances.

The practical engine, especially the one for motorcycle is designed to gain the highest performance in the power, the fuel consumption rate and the exhaust gas controlling within the limitation of dimensions. For example, in case of the pressure loss at the suction not to be allowed, the combustion improvement by adopting the shroud or the helical port is not always the best selection considering its total balance of the performance at the operational conditions.

During driving in the urban area, the ratio of idling to cruising times becomes larger. So that the improvement of engine performance at idling operation becomes important from the standpoints of pollution control and fuel economy.

By such a background the authors have paid attentions to the real phenomena happening inside the commercial spark ignited engine from the fundamental point of view. An air-cooled, four-valved, 250 ml motorcycle engine was used as a test engine. Laser Doppler anemometer was used to measure the time averaged flow velocity and rms value of velocity fluctuation distributions inside the cylinder under the motoring conditions. The results are compared with the direct photographs of engine flames in order to understand how the flow pattern induced during the suction and compression strokes affects the combustion characteristics.

EXPERIMENTAL APPARATUS AND PROCEDURES

An air-cooled, four-valved, 250 ml Suzuki motorcycle engine was used. The specification of which is shown in Table 1. Fig. 1 shows the valve locations and valve timing. Inlet valve starts to open at 28° BTDC and close at 52° ABDC. Exhaust valve starts to open at 60° BBDC and close at 20° ATDC. So that both valves open with overlapping from 28° BTDC to 20° ATDC.

The valve angle of the tested engine is rather narrower (26° half angle) than an ordinary

* Graduate School Student sent from Suzuki Automobile Co., Ltd.

** Professor

*** Professor, Visiting Researcher to Toyohashi University of Technology from April 17 to June 16, 1984

Table 1 Specifications of Tested Engine

Bore (mm)	72
Stroke (mm)	62.1
Compression Ratio	8.9 (normal) 3.5 (experimental)
Valves	dual (normal) dual and single (experimental)

four-valved engine and the intake port shapes rather straight. So that the swirl component of the intake gas could not be expected and in this experiment the attention was paid to measure the velocity component along the piston stroke.

A laser Doppler anemometer measures the velocity distribution in the cylinder. In order to introduce the laser beams of anemometer into the cylinder, following two methods were adopted.

Firstly the iron spacer on which quartz windows were mounted, through which the laser light was

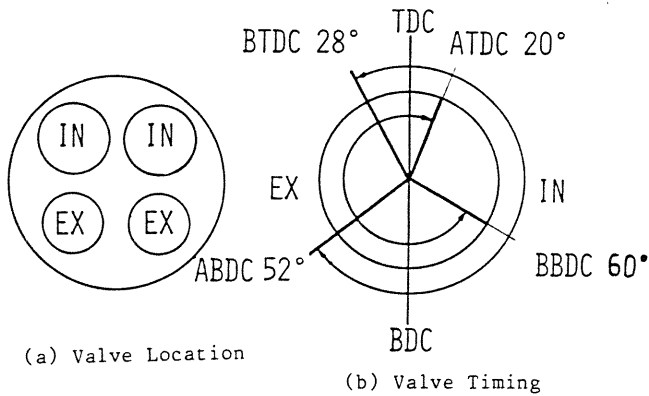
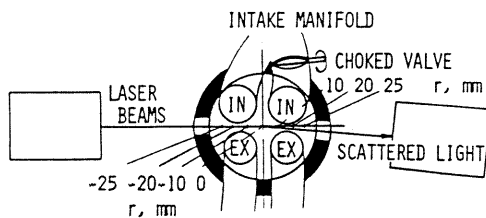
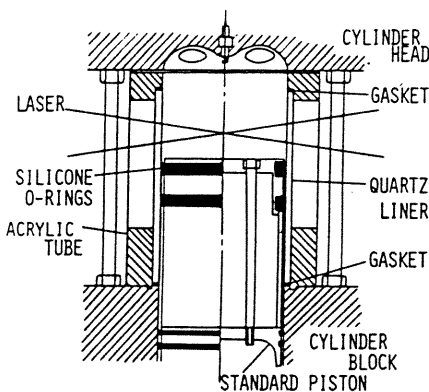


Fig. 1 Valve Location and Timing



(a) Iron Spacer



(c) Quartz Cylinder

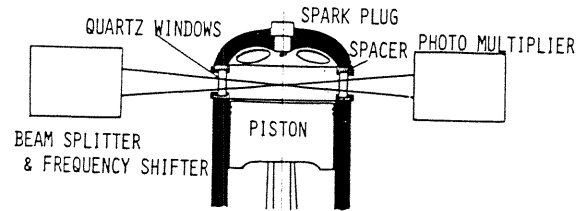
introduced, was inserted between the cylinder and its head. Secondly the quartz cylinder fitted inside the acrylic resin tube was used in place of the engine cylinder. In this case, the laser beams were introduced through the slits cut on the resin tube. The quartz cylinder was designed not to be compressed axially, but to be airtightened. The spacer was used to measure the velocity near valves and the cylinder to cover the wider regions along the piston movement. The details are shown in Fig. 2.

JIS No. 8 standard fine powder or sprayed salad oil droplet was used as the scattering particle for the laser Doppler anemometer.

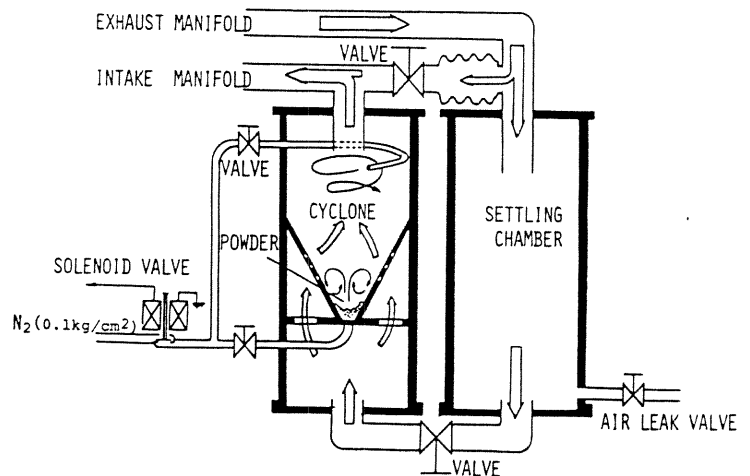
Powder was used when the spacer was adopted. It was agitated inside a cyclone type powder supplier by the circulating air flowing through the closed loop, and floated in its stream and introduced into the cylinder when a solenoid valve was opened to synchronize the data to the crank angle to be measured. If the powder was introduced all the time, the quartz window would be dimmed by the powder and S/N ratio of the obtained signal became very low and the velocity could not be measured. The exhausted gas was returned to the powder supplier and the powder could be recirculated. Pressure was released to the outside through the valve as shown in Fig. 2.

The oil was adopted when the quartz cylinder was used, since if the powder is introduced in the case of cylinder, inside surface is dimmed by the powder and scratched by the piston ring. Silicone O-rings were used as the piston rings in the case of quartz cylinder. An upper O-ring holds the function of a wiper as well and high S/N ratio signal can be obtained.

A He-Ne 20 mW laser and all the optical components of the laser Doppler anemometer were



(b) Location of Laser Beams of LDA



(d) Powder Supply System

Fig. 2 Experimental Apparatus

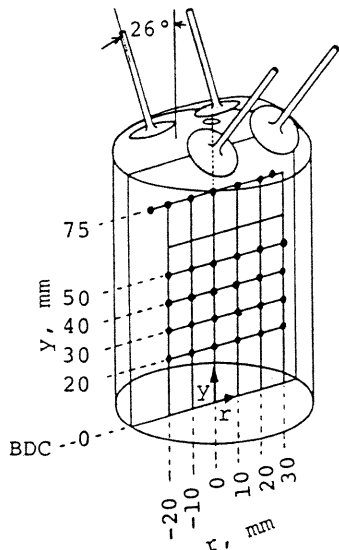


Fig. 3 Measured Points

aligned on the optical platform supported by the precision pantographs and traversed both horizontally and vertically. The measured points are shown in Fig. 3.

The Doppler signal was converted into the velocity by a counter system. A frequency shifter was used to determine the flow direction. Thus obtained data was recorded PCM data recording system with crank angle detected by a conventional optical devices. The recorded data was analyzed by a personal computer system.

The compression ratio became 3.5, since the spacer was introduced. The height of the cylinder and the piston stroke in case of quartz cylinder were selected such that the same compression ratio could be realized.

Fig. 4 shows all the apparatus said above, in which the quartz cylinder is used.

Other than the above said experiment, the direct photographs of flame propagation under the firing conditions were taken by a still camera, the shutter chance of which was synchronized with the crank angle by an electronic controlling circuit. In this case an engine shown in Fig. 5 was used. The head of the specially designed long piston as shown in the figure was

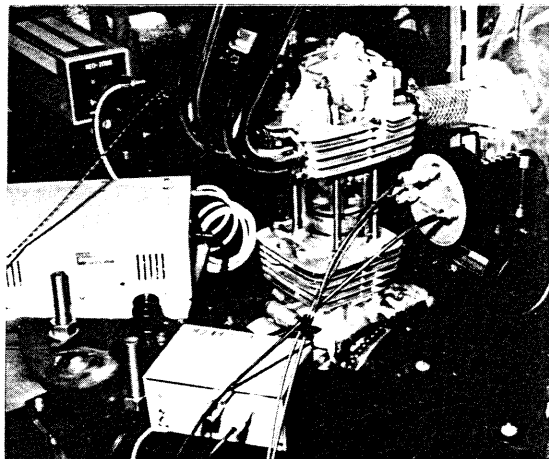
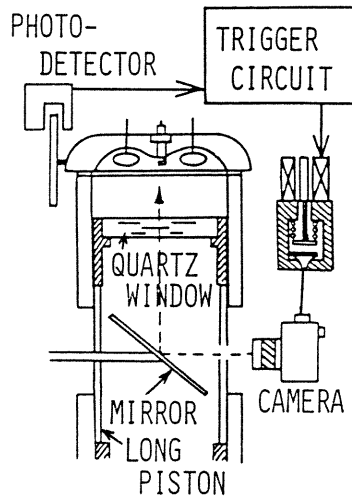
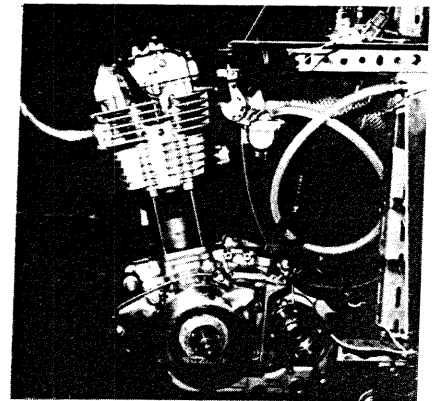


Fig. 4 Whole View of Test Rig



(a) Schematics



(b) External View

Fig. 5 Quartz Piston Head Engine to observe Flame Propagation

constructed by a quartz window, through which the cylinder could be observed. A 43mm x 46mm surface mirror was set in 45° within the cylinder vacancy to reflect the sight inside the cylinder to the outside through the hole constructed on the side of the piston.

RESULTS AND DISCUSSIONS

Momentum and Velocity of Intake Air

150, 300 and 600 rpm, full and half throttled single and dual intake valve operations were selected as the experimental conditions. In order to understand the relations between the piston motion and intake air flow during the suction stroke, intake air velocity and its momentum at the intake manifold were calculated by the Gas Exchanging Simulation Code. The results at full throttled and 600 rpm are shown in Fig. 6 with piston position and its velocity. The air velocities at the intake valve gap in case of dual and single intake valve operations at full throttled condition calculated from the above said intake velocity at intake manifold are also shown in the same figure. It can be observed in case of the single intake valve operation that the intake air at the valve gap chokes just after the intake

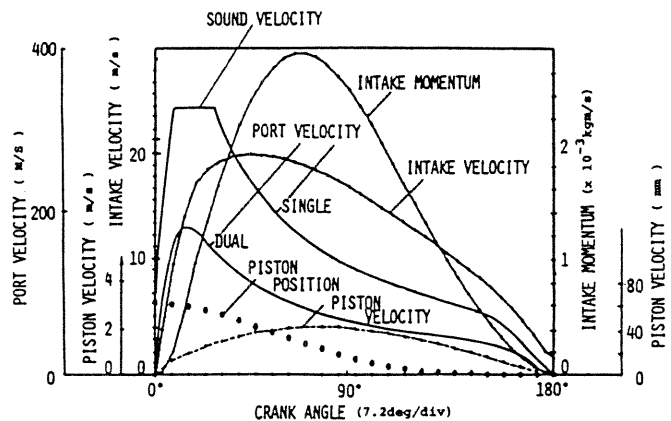


Fig. 6 Momentum and Velocities of Intake Air

valve opens. Intake air velocity at the valve gap during the suction stroke other than this choking duration in the case of single valve operation is twice as high as that of dual valve.

Flow Velocity Near Intake Valve

Dual Valve Operation

In order to discuss the flow induced by the intake air, velocity near the intake valve was measured with using the spacer. The ensemble averaged time mean velocity and velocity fluctuation over 50 cycles are mapped on the plane of the distance along the diameter versus the crank angle.

The result of time mean velocity at the dual valve operation, 600 rpm and full throttled conditions is shown in Fig. 7. Velocity at suction stroke is shown in (a) of the figure and that at compression in (b). In the figure, 0 mm corresponds to the center of the cylinder and plus and minus signs and distance are as defined in Fig. 3. In both figures left hand side corresponds to TDC and right hand does to BDC and one division does to the crank angle of 7.2° . The length of horizontal arrow shows the magnitude of velocity and the direction of arrow does the flow direction. The magnitude of 1 m/s is shown at right bottom of the figures. The base lines are inclined slightly so that the arrows do not interact with each other.

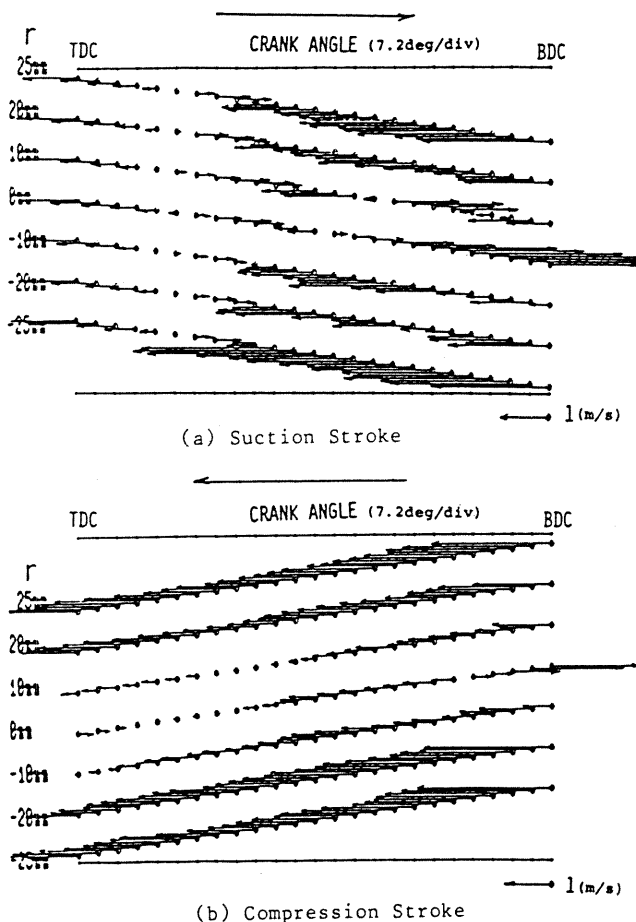


Fig. 7 Time Mean Velocity at Dual Valve, 600 rpm, Full Throttled Operation at $y=75$ mm

Since the momentum of the discharging air flow is strong and exhaust valve still opens slightly until 20° ATDC, the upward flow remains at the beginning of suction stroke. This upward flow decays by the interaction with the intake air flow and the downward flow starts in the whole cross-sectional area at around 35° ATDC.

Soon after this timing, the strong interaction between two conical inclined intake air jets produces downward flow near the center during the rest of suction stroke and it changes into upward one soon after the compression stroke starts. While in the suction stroke upward flow occupies almost off-center region as the result of recirculations behind the intake valves, the magnitude of which becomes larger near the cylinder wall. It is well expected that the another downward flow is induced near the cylinder wall surface by the intake air. This results the double toroidal vortex type circulations being induced near the cylinder head.

The upward flow at the off-center region during the compression stroke is kept almost constant after the central flow changes its direction.

The velocity fluctuation at the same working condition, on the other hand, is shown in Fig. 8. Velocity fluctuation along the diameter does not seem to have so much difference. It decays during the expansion stroke, increases when the moving direction of the piston changes at BDC and again decays during the exhaust stroke. The sources of increasing the velocity fluctuation after the suction stroke starts are different from those observed above. The intensive shear flow formed by the intake air is the main source of producing the turbulence in this case. The magnitude of the velocity fluctuation is larger than that observed at former strokes. The point at which the velocity fluctuation has its maximum almost corresponds to the starting point of downward flow at the center of cylinder and also does to the maximum point of momentum of intake flow, not velocity. During the suction stroke the production rate of the turbulence exceeds or equilibrates the decay

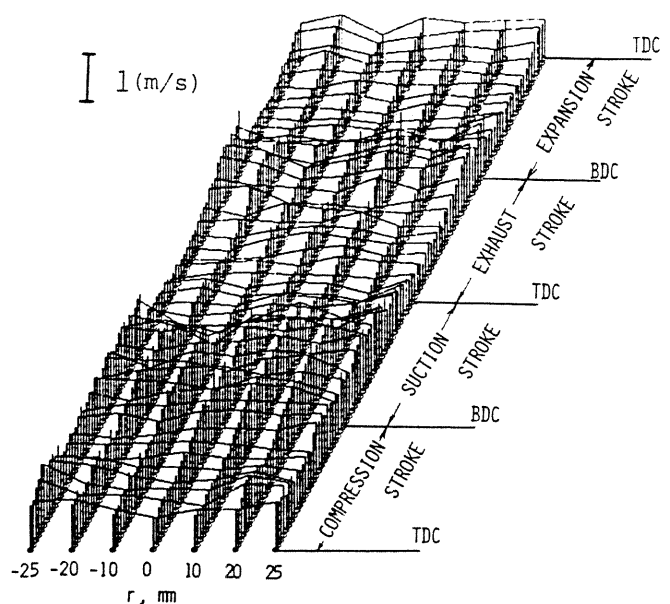


Fig. 8 Velocity Fluctuation at Dual Valve, 600 rpm, Full Throttled Operation at $y=75$ mm

rate, so that the velocity fluctuation can keep its magnitude. The upward mean flow appeared during the compression stroke shown in Fig. 7 could produce the turbulence at the shear layer formed between the flows of different velocities and the decay rate of velocity fluctuation is not so steep on an average as observed in the figure. In this sense the turbulence is produced near the wall surface, while it decays at the central part.

At the half throttled operation with other conditions being kept same as those of full throttled, the time mean velocity distributions become different from those at full throttled as shown in Fig. 9. The most different point is that the duration of remaining the downward flow across the cross-sectional area in the suction stroke becomes longer but the downward flow at the central part of cylinder disappears and almost of all the flow indicated in the figure directs upward after about 80° ATDC. So that during the suction stroke, downward flow exists only near the cylinder wall region and a single large toroidal vortex type circulation strongly appears until the middle part of the compression stroke and then the vortex steeply damps. This kind of flow patterns are realized by the slower intake velocity and the flow penetrating into the middle part of the cylinder becomes weaker than the full throttled case.

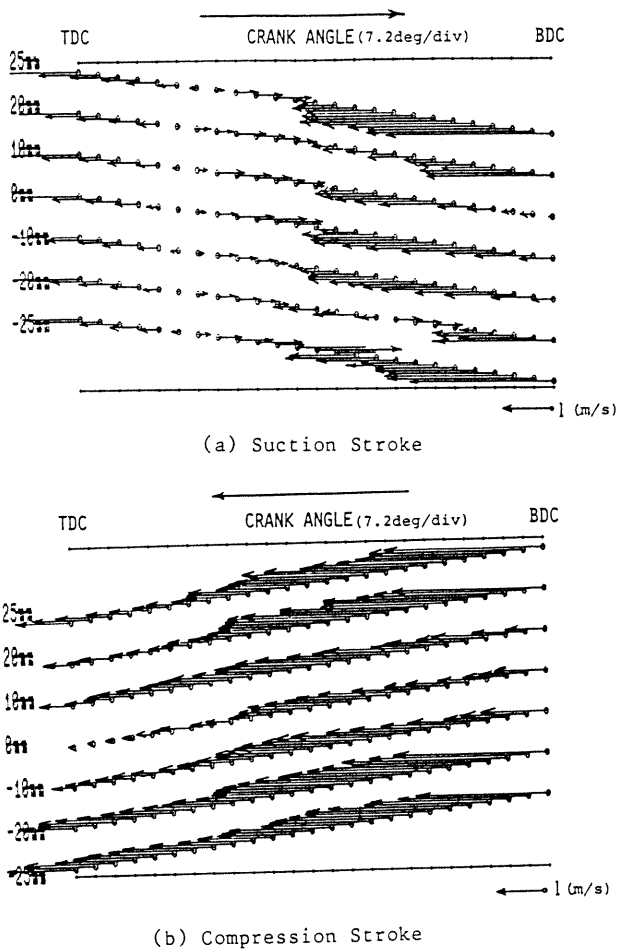


Fig. 9 Time Mean Velocity at Dual Valve, 600 rpm, Half Throttled Operation at $y=75$ mm

Single valve Operation
The results at the single valve operation, 600 rpm and full throttled condition are shown in Figs. 10 and 11 by the same fashions as in the

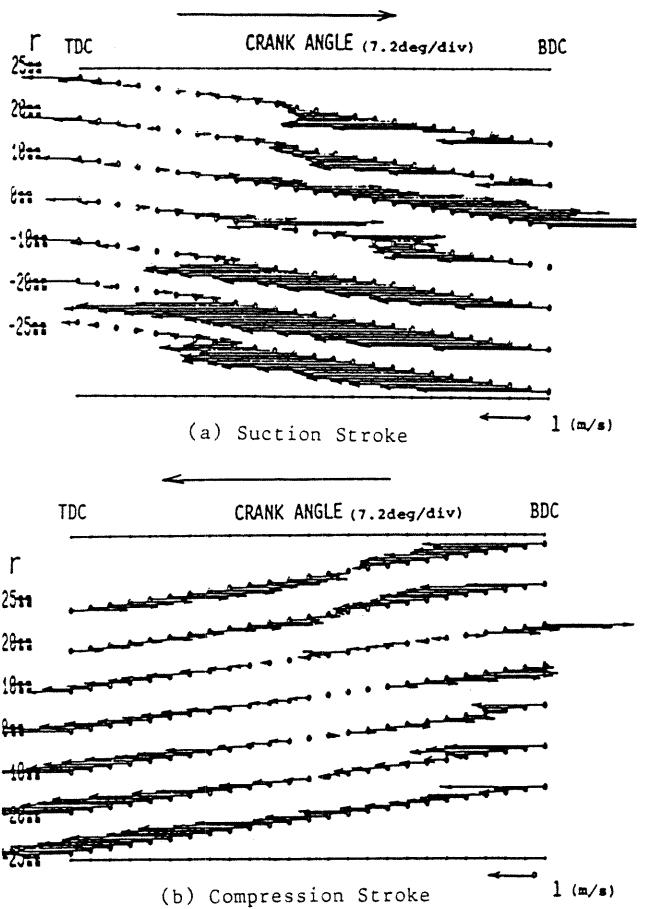


Fig. 10 Time Mean Velocity at Single Valve, 600 rpm, Full Throttled Operation at $y=75$ mm

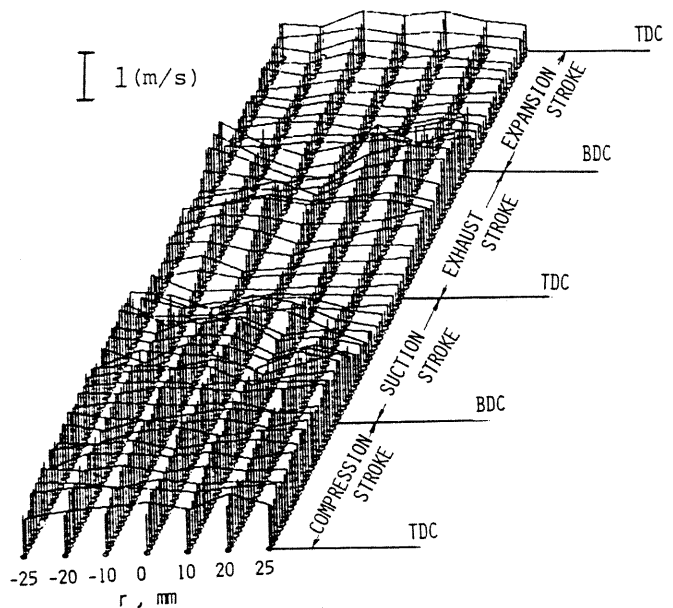


Fig. 11 Velocity Fluctuation at Single Valve, 600 rpm, Full Throttled Operation at $y=75$ mm

above two figures. In this case the flow changes into asymmetric, but still has the duration that all the flows direct downward after the flow direction changes at the early stage of the suction stroke. After this duration, double toroidal vortex type circulation appears until the middle part of the compression stroke. After the middle of the compression stroke the downward flow near the center changes its direction and at the same time the upward flow near the wall at positive r changes its flow direction into downward. After this time the toroidal flow changes its shape into a single roll vortex. In this case the general tendencies of production and decay of the velocity fluctuation during expansion and exhaust strokes are the same as the former case, but it can be well observed that the flow pattern affects the timing and the positions of increasing the

velocity fluctuation. At the suction stroke air is introduced from the valve located in the negative r region and the production of velocity fluctuation proceeds in this region than in the positive r . After the middle of compression stroke a shear flow appears at the central part by forming a single vortex and the decay of velocity fluctuation in this region is not realized in this case.

In the case of half throttled operation of single valve at the same speed, the flow pattern realized was a little weaker but almost as same as that of full throttled. This can be considered as the downward flow at the central part, though the magnitude is less than that at full throttled, can still induce the dual vortex. The figure is omitted for want of space.

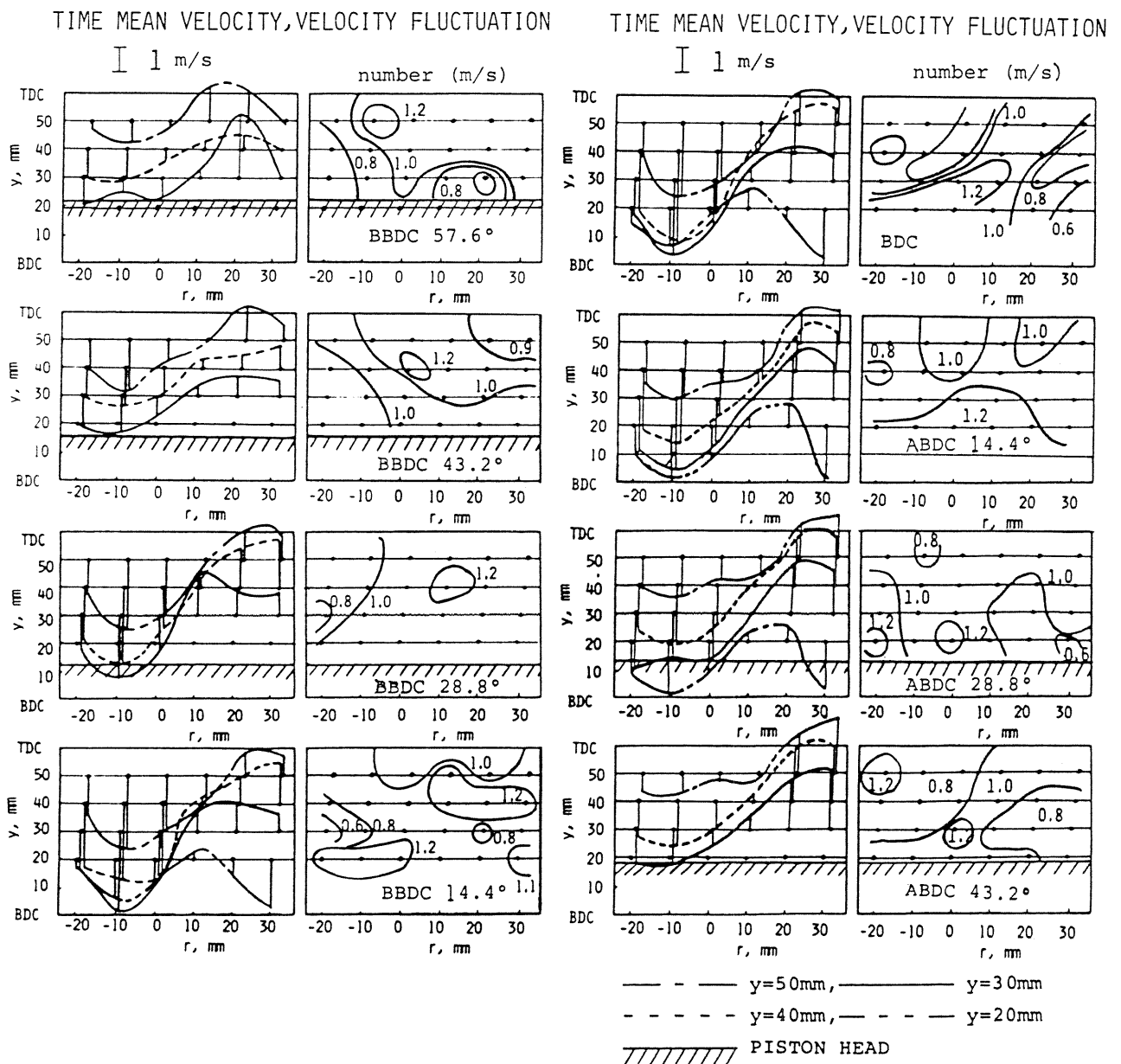


Fig. 12 Flow Pattern of Time Mean Velocity and Velocity Fluctuation at Dual Valve, 600 rpm, Full Throttled Operation

Flow Pattern on the Center Plane in the Cylinder

The data obtained at the measuring grid points shown in Fig.3 was calculated every 7.2° crank angle and the time mean velocity and velocity fluctuation were illustrated on the plane of radial distance versus height of stroke. The typical results picked up from the series of graphs of dual valve operation, 600 rpm and full throttled condition are shown in Fig. 12.

The downward flow induced at the central part mentioned in Fig. 7 changes its direction between $y=75$ mm and 50mm from the center to the off-central part of minus r region and strong single vortex occupies the cylinder other than the cylinder head region until the end of compression stroke. This kind of deflection of flow may happen by the slight unbalance of the momentums of two conical air jets and the jet in plus r region

wins the other one. Combining the results of Figs. 7 and 12, the flow in the cylinder is considered to be divided into two parts, one is the symmetric dual toroidal vortex near the cylinder head region and the other is a strong single vortex in the remainder.

The contour of velocity fluctuation on the other hand shows the turbulence is produced at the region of steep velocity gradient, but the magnitude of the fluctuation is not so large as in the other case. This shows that the existing steady and big vortex has less effect on producing the strong turbulence.

The results of 300 rpm with other operational conditions being same as Fig. 12 is shown in Fig. 13. Until the middle part of suction stroke, the flows at $y=40$ and 50 mm seem to be symmetric, but near BDC the flows begin to have the same tendencies shown in Fig. 12. On the other hand

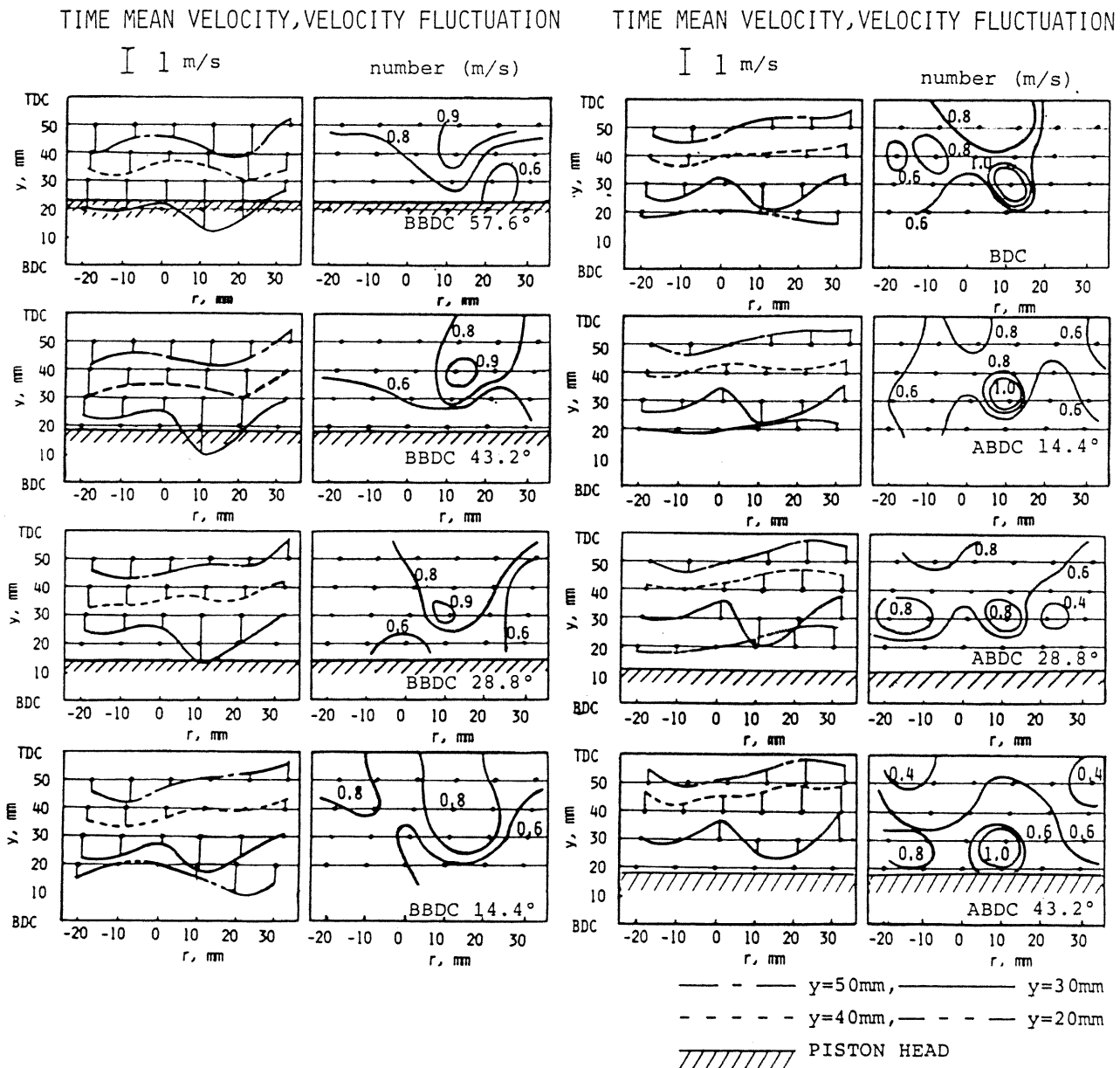


Fig. 13 Flow Pattern of Time Mean Velocity and Velocity Fluctuation at Dual valve, 300 rpm, Full Throttled Operation

the flow at $y=30$ mm seems to have the amplified shape of the flow at $y=40$ mm. The reflection of the flow on the piston head has the great effect on this tendency. In the compression stroke, the shapes of the flows at $y=40$ and 50 mm are similar to those in Fig. 12, but in this case the flows direct upward.

The distribution of velocity fluctuation is a little different from the former result. In this case shear force is produced not only in r but in y direction, especially between $y=30$ and 40 mm. So that the highest fluctuation locates in this region.

Very different and strong circulations were realized at the single valve operation at 300 rpm, full throttled. The results are shown in Fig. 14.

Only the suction valve located in minus r region operated. Since the intake air momentum becomes four times as high as that at dual valve operation, the penetration of the conical jet into the cylinder becomes stronger and the flows having two peaks of downward flow at $y=40$ and 50 mm were realized at around 70° to 80° BBDC. The flow at $y=30$ mm shows the effect of reflection on the piston head and shapes strong vortex. During the compression stroke, the flow directs upward, but it still remains the flow patterns experienced in the suction stroke.

The velocity fluctuation in this case was the most strong, because the steep velocity gradients appear between $y=30$ and 40 mm in the suction stroke and $y=20$ and 30 mm in the compression.

At father slower engine speed of 150 rpm, in

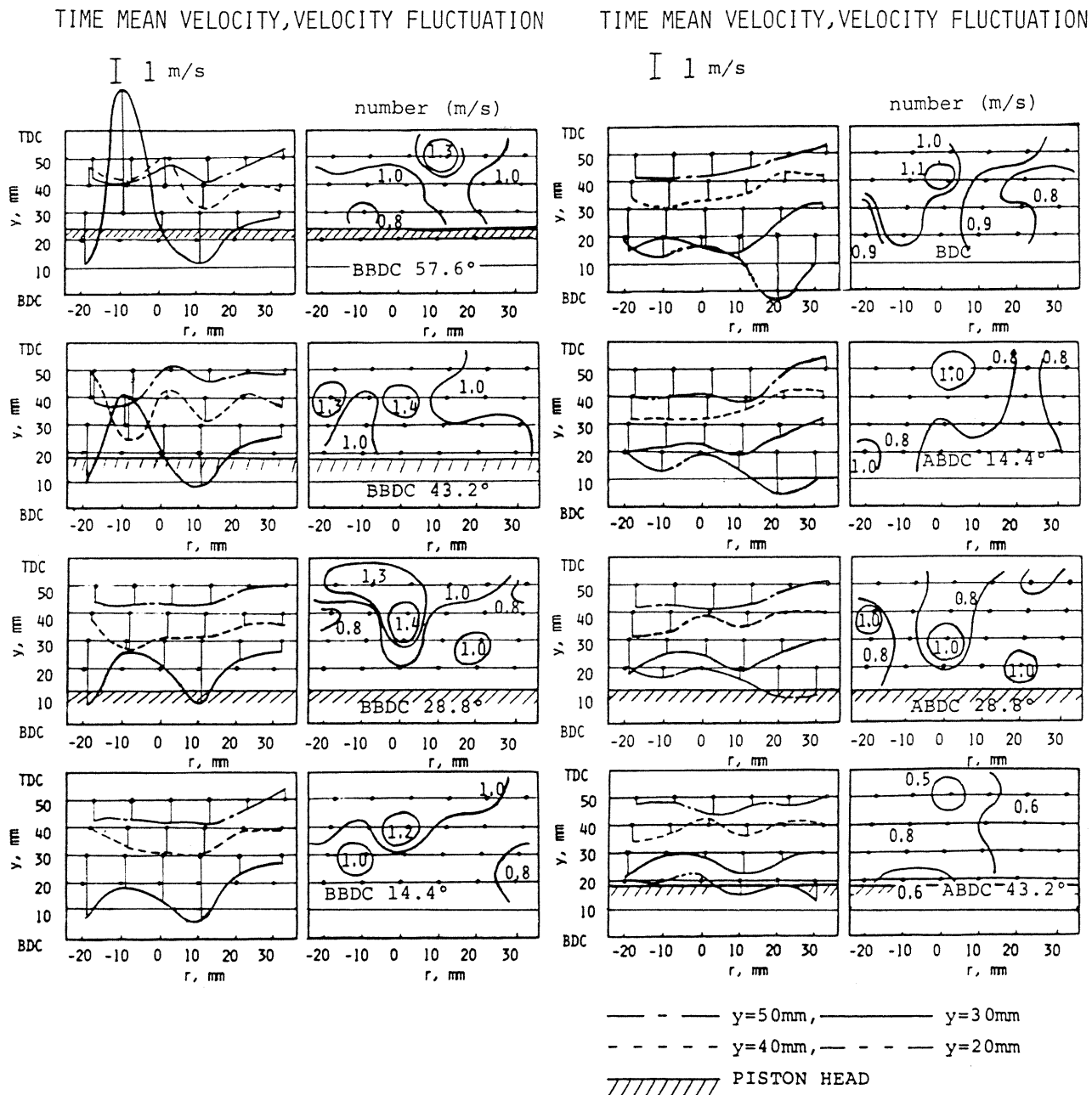


Fig. 14 Flow Pattern of Time Mean Velocity and Velocity Fluctuation at Single Valve, 300 rpm, Full Throttled Operation

both dual and single valve operations, with full throttled the intake momentum of the introduced air becomes the smallest among the tested cases and the inertia of the conical jet of the intake air flow is not so strong as that at higher speeds. The result, not shown for want of space, clearly reflects this characteristics and the flow at around BDC, the timing of suction stroke changing into compression stroke, almost follows the piston movement. At the middle stage of the suction stroke, at around 70° BBDC, flow pattern across the diameter has two-peak shape as the result of dual valve operation. In the compression stroke almost of all the flow are induced by the piston movement and the flow during the suction stroke almost loses its effect.

The magnitude of velocity fluctuation is the smallest among these three cases and almost uniform.

DIRECT PHOTOGRAPHS OF ENGINE FLAMES

The direct photographs of engine flames colored by JIS No.8 standard fine powder were taken by the specially assembled engine as shown in Fig. 5. Kodak Tri-X film was used and exposure time and f number were $1/1000$ second and 1.4 respectively. During this exposure time the engine runs 7.2° at 1200 rpm.

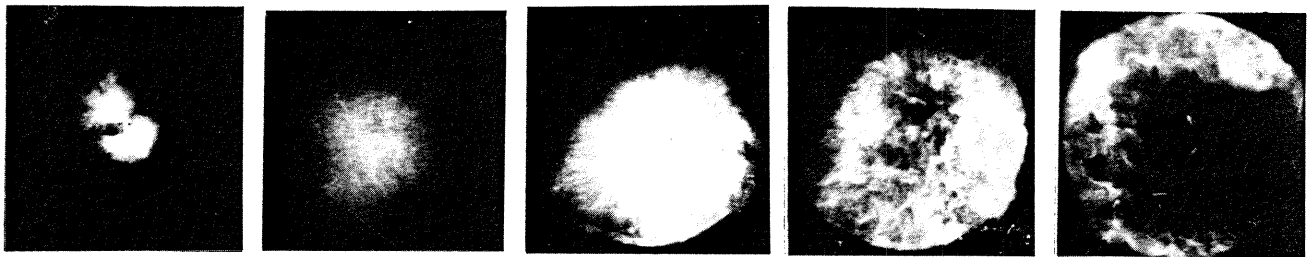
Thus taken photographs are shown in Fig. 15, in which (a) corresponds to the dual valve operation and (b) to the single. Though the range of engine speed is different from those at velocity measurements, the characteristics of the flow pattern might be similar to those at higher engine speed among tested. Higher momentum flow at single valve operation would give the stronger mixing to the combustible mixture than the dual operation. The photograph well describes this characteristics and the combustion takes place uniformly propagated from center to outside at the single valve operation, while at the dual valve, combustion starts from the peculiar region and non-uniform propagation and combustion take

place. A 1200 rpm is a slower idling speed as a motorcycle engine, so that it can be said that the single valve operation is effective to improve the idling engine performance.

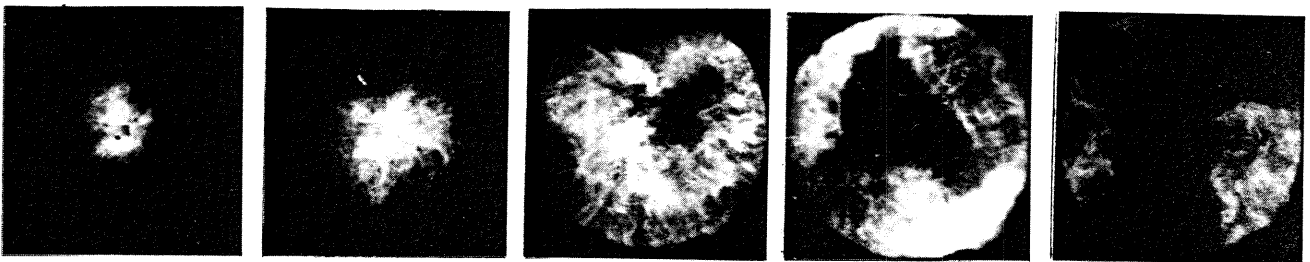
CONCLUSIONS

As the results of flow pattern measurements and observations of flame propagations by direct photographs, the following conclusions can be obtained.

- 1) By the dual valve operation, the double toroidal vortex occupies the volume near cylinder head and maintains its shape until for a while after compression stroke starts. The stronger is the tendency, the higher the engine runs.
- 2) The flow pattern formed under this vortex depends on the momentum of the intake air flow. At the higher flow momentum, the interaction of the dual conical air jets decides the flow pattern and even at the dual valve operation a single vortex can be formed as the result of competition.
- 3) The velocity fluctuation steeply increases after the suction of fresh air starts and almost maintains its magnitude during the suction stroke. The magnitude is almost uniform across the measured diameter and decays slowly during the compression stroke.
- 4) At the single valve operation, the double, but asymmetric toroidal vortex appears and maintains its shape until almost the same crank angle as the dual valve operation. The velocity fluctuation also shows almost the same tendency mentioned above. Only the difference is the locations where it increases its magnitude. It is affected by the eccentricity of the flow.
- 5) The production of turbulence is well explained by the velocity gradient and affects the flame propagation in cylinder.
- 6) Direct photographs of flames show that the mixing has the great effect on the characteristics of flame propagation and single valve operation shows better combustion performance at rather low idling speed.



(a) Dual Valve Operation at 1200 rpm



(b) Single Valve Operation at 1200 rpm

Fig. 15 Direct Photographs of Propagating Flames in Cylinder
Ignition Timing : 10° BTDC, A/F Ratio : 14

ACKNOWLEDGMENT

The authors would like to express their thanks to Mr. T. Ida, Mr. Y. Deguchi and Mr. H. Abe for their voluntary helps in taking, developing and printing the direct photographs of engine flames and computer calculation.

REFERENCES

1. Ekchian, D. and Hoult, D. P., "Flow Visualization Study of Intake Process of an Internal Combustion Engine", SAE Trans., Vol. 88, pp.383-400, 1979.
2. Hirotsu, T., Nagayama, I., Kobayashi, S. and Yamamasu, M., "Study of Induction Swirl in a Spark Ignition Engine", ibid, Vol. 90, pp.1851-1868, 1981.
3. Namazian, M., Hansen, S., Lyford-Pike, E., Sanchez-Barsse, J., Heywood, J. and Rife, J., "Schlieren Visualization of the Flow and Density Fields in the Cylinder of a Spark-Ignition Engine", ibid, Vol. 89, pp.276-303, 1980.
4. Dent, J. C. and Derham, J. A., "Effects of Engine Variables on Turbulence in a Spark Ignition Engine", SAE Paper No. 760159, 1976.
5. Waguri, Y., Kido, H., Ono, S., Nakashima, K. and Murase, E., "Influence of Swirl and Turbulence on the Burning Velocity in an Engine Cylinder (2nd Report, Experiment with Single-Compression Test Equipment)", Trans. of JSME, Vol. 46, No. 406, B, pp 1184-1193, 1980.
6. Rask, R. B., SAE Paper, No.970094, 1979.
7. Matsuoka, S., Nagakura, K., Kawai, T., Aoyagi, Y. and Kamimoto, T., "Application of Laser Doppler Anemometry to a Motored Diesel Engine" Trans. of JSME, Vol.47, No. 422, B, pp.2074-2084, 1981.
8. Dunn-Rankin, D., Chen, R. K., and Sawyer, R. F., "LDA Study of Non-steady Flame Propagation in a Closed Duct", LDA Conference, Lisbon, July, 1984.